Optical and Quantum Electronics (2022) 54:860
https://doi.org/10.1007/s11082-022-04258-7

Energy spectrum and interlevel transitions within the conduction band of a D_2^+ complex confined in a spherical quantum dot

E. B. Al[1] · H. Sari[2] · S. Sakiroglu[3] · I. Sökmen[3]

Received: 21 October 2021 / Accepted: 27 September 2022

Abstract
In this work, we have performed a theoretically study on the energy spectrum, binding energy and interlevel transitions within the conduction band of a D_2^+ complex confined in a spherical quantum dot with finite confinement potential by using diagonalization method within the effective mass approximation. We analyzed the effect of the quantum dot size and internuclear distance on the binding energy, equilibrium distance and optical response of the singly ionized double donor complex. Theoretical analysis of the D_2^+ system indicated that the internuclear distance significantly affects the energy difference between the two lowest-lying electron states and amplitude of the interlevel transitions within the conduction band. In general, the internuclear distance and quantum dot size dependence of the energy states of the D_2^+ complex in a quantum dot shows that the optical sensitivity of a quasi-two-level system can be tuned as desired.

Keywords Quantum dot · Impurity · Molecular complex · Optical transitions

1 Introduction

In recent years, investigation of electronic and optical properties of low-dimensional semiconductor systems in which carriers' movement freedom is restricted has gained importance. In this context, many studies have been carried out to determine the basic properties of quantum dots (QDs), also called artificial atoms (Bednarek et al. 1999; Cheng et al. 2003), in which the particles are confined in three directions. This strong confinement in QDs gives them unique properties and allows them to be considered as ideal systems for

I. Sökmen: Retired.

✉ H. Sari
sari@cumhuriyet.edu.tr

[1] Faculty of Science, Physics Department, Sivas Cumhuriyet University, 58140 Sivas, Turkey

[2] Faculty of Education, Department of Mathematics and Natural Science Education, Sivas Cumhuriyet University, 58140 Sivas, Turkey

[3] Faculty of Science, Physics Department, Dokuz Eylul University, 35390 Izmir, Turkey

Published online: 22 October 2022

next generation optoelectronic devices such as lasers, photodetectors, amplifiers and solar cells.

Up to date, the studies have shown that the electronic structure and optical response of impurity trapped in these zero-dimensional structures exhibits interesting properties (Bimberg et al. 1999; Wu et al. 2015; Pavlović 2016; Bera et al. 2016; Abolfath 2009; Ghosh et al. 2016). For instance, in the study on the current progress in III–V QD based optoelectronic devices by Wu et al. (2015), it was stated that doping in the active region plays a critical role in the performance of QD infrared photodetectors. The energy spectrum and corresponding eigenfunctions of the hydrogenic donor confined in a square QD is investigated by Pavlović in a four level ladder configuration (Pavlović 2016). The obtained results are used to analyze the effects of the confinement and the laser field on the electromagnetically induced transparency and it is emphasized that the absorption peak width is a non-monotonic function of the confinement of the hydrogenic impurity. On the other hand, Bera et al studied the modulation of electro-optical effect and nonlinear optical sensitivity of the impurity doped QD in the presence of noise with Gaussian distribution (Bera et al. 2016). In their study, it was noted that the effect of dopant location could hardly be observed in the absence of noise and in the presence of additive noise. Nonlinear optical responses of doped QDs have been performed by Ghosh et al in presence of Gaussian white noise with fixed and spatially varying effective mass by modelling the impurity potential via a Gaussian function (Ghosh et al. 2016). In their work, it is emphasized that the noise effect on the nonlinear optical response becomes more pronounced for the spatially varying effective mass case.

Advances in the single-doping technique (O'Brien et al. 2001; Schofield et al. 2003; Shinada et al. 2005) and charge detection (Schoelkopf et al. 1998; Aassime et al. 2001) have led to increased interest in another molecular system consisting of two confined donor impurities in a semiconductor host where one of the two excess electrons is ionized. Certainly, the ability to control the location of individual dopant atoms within a semiconductor heterostructures has enormous potential for creation atomic-scale electronic devices. Current techniques for controlling the spatial extent of dopant atoms rely on either ion implantation techniques or dopant diffusion through optical or electron-beam patterned mask layers. In addition to these known conventional techniques, different new methods have also been developed which offer a new path toward the creation of atomic-scale electronic devices (Schofield et al. 2003; Matsukawa et al. 1997; Shinada et al. 2000, 2002, 2006). For instance, Schofield et al. present a work to position P dopant atoms with atomic precision by using scanning tunneling microscopy-based lithography on H passivated Si(001) surfaces to control the adsorption and subsequent incorporation on single P dopants into the Si(001) surface (Schofield et al. 2003). They demonstrated the positioning of single atoms in Si with accuracy and the creation of nanometer wide lines of incorporated P atoms. Shinada et al. reported the fabrication of semiconductors with both dopant number and position controlled by using a one-by-one doping technique called single-ion-implantation (Shinada et al. 2006). In this technique, single ions are extracted by chopping a focused ion beam using a high frequency beam deflection and the number of implanted ions is controlled one-by-one by detecting secondary electrons emitted from a target upon a single ion incidence. They emphasized that if one can precisely control the dopant distributions, significant improvements in device properties can be achieved for successful future semiconductor electronics. Further, a great deal of experimentally (Fuhrer et al. 2009; Makkara and Viswanatha 2018) and theoretical (Du et al. 2008) effort has been devoted to obtaining QDs with high dopant concentrations as well as single dopant regimes. Careful control of parameters such as the dopant core size, core lattice strength, and temperature can lead to

effective doping. The types of dopant precursors and their lattice strength play an important role in the aforementioned doping technique. Although the controlled incorporation of dopants into QDs has made great progress in recent years, it remains a frontier issue in doping chemistry. In this context, the studies on the electronic structure and related properties of H_2^+-like impurities confined in QDs have been carried out (Kang et al. 2008a, b). Particularly, Kang et al have introduced a variational method to calculate the energy spectra of the H_2^+-like impurities confined by spherical QDs as a function of the nuclear distance for different geometric sizes of the structure (Kang et al. 2008a). In this study, a quantitative analysis of the ground and some low-lying energy states is presented. In another study, they proposed a scheme for realizing a charge qubit consisting of ground and first excited states of a confined double-donor system by spherical $GaAs - Ga_{1-x}Al_xAs$ QDs (Kang et al. 2008b). They have found that under suitable physical conditions, H_2^+-like impurities confined in QDs can be considered as a quasi-two-level system, and the localized impurity states of this system can be used as charge qubits. This two-level system encodes logical information on the spin or charge degrees of freedom of a single electron and allows us to tune its molecular properties accordingly (Calderón et al. 2007, 2006; Hollenberg et al. 2004; Tsukanov 2007; Openov 2004; Koiller et al. 2006; Barrett and Milburn 2003). The effect of spatial and dielectric confinements on the electron charge distribution, spontaneous emission rates, and transition energies of a singly ionized double donor system (D_2^+) in a QD are calculated by Movilla et al using the effective-mass approximation (Movilla et al. 2009). They reported that the confinement of the D_2^+ system in a QD provides additional possibilities to tune its properties such as the charge distribution of the lowest-lying states, the corresponding energy splittings, and the radiative lifetimes. The energies and eigenfunctions of a singly ionized D_2^+ complex in vertically coupled QDs in the presence of a magnetic field were calculated by Manjarres-Garcia et al using a variational separation of variables for different structure morphologies (Manjarres-García et al. 2012). Recently, Xu and colleagues performed a pump-probe experiment to investigate electron localization in the dissociation of the H_2^+ molecule and breaking a chemical bond in real time (Xu et al. 2017). The experimental results obtained in their studies were also supported by a theoretical simulation based on the numerical solution of the time-independent equation.

Motivated by the importance of coupled donor impurities in nanotechnology applications, in this study we focus on the energy spectra, binding energy and intersubband optical absorption of a D_2^+ molecular complex confined in a spherical quantum dot with finite confinement potential. We investigate the effect of both the nuclear distance and the QD size on the energy spectra, the binding energy, the molecular dissociation energy and optical absorption coefficients (OACs).

The present study is organized as follows: In Sect. 2, we introduce the physical model of the singly ionized D_2^+ complex confined in the QD and outline the details of the numerical method used to solve the resulting eigenvalue equation. The obtained results are presented and discussed in Sect. 3, and our conclusions are given in Sect. 4.

2 Theoretical framework

2.1 D_2^+ complex

In the framework of the effective mass and parabolic band approximation, the Hamiltonian of the D_2^+ complex in the spherical QD can be written as

$$H = -\frac{\hbar^2}{2m^*}\nabla^2 + V_{QD}(r) + V_{DD} + V_C\,, \tag{1}$$

where m^* is the effective mass of the electron in the QD material, r is the distance from the electron to center of QD. For simplicity, we assume that one of the two positive donors is located at the center of the $GaAs/Ga_{1-x}Al_xAs$ QD and the other donor is located at the D-position on the z-axis. $V_{QD}(r)$ is the spherically symmetric confinement potential and it is defined as Al et al. (2021)

$$V_{QD}(r) = \begin{cases} 0, & r < R \\ V_0, & r \geq R \end{cases}, \tag{2}$$

where $V_0 = Q_c\Delta E_g$ is the barrier height, R is the QD radius, $Q_c = 0.6$ is conduction band offset parameter and $\Delta E_g = 1247x\,(meV)$ (Adachi 1985) is the difference between the band gaps of $Ga_{1-x}Al_xAs$ and $GaAs$ QD materials and depends on the aluminum alloy concentration (x) in $Ga_{1-x}Al_xAs$.

V_{DD} is the donor-donor repulsive Coulomb potential and it is written as

$$V_{DD} = \frac{e^2}{\varepsilon D}, \tag{3}$$

where e is the absolute value of the electronic charge and ε is the effective dielectric permeability of the QD.

V_C is the attractive Coulomb interaction potential between electron and donors and it is given by

$$V_C = -Z\frac{e^2}{\varepsilon}\left(\frac{1}{|\mathbf{r}-\mathbf{D}|} + \frac{1}{r}\right), \tag{4}$$

where $Z = 0$ ($Z = 1$) indicates the case without (with) electron-donor interactions.

The term $\frac{1}{|\mathbf{r}-\mathbf{D}|}$ is given in terms of spherical harmonics by

$$\frac{1}{|\mathbf{r}-\mathbf{D}|} = \sum_{\mu}\frac{4\pi}{2\mu+1}f_\mu(r)\sum_{\nu=-\mu}^{\mu}Y^*_{\mu,\nu}(\theta,\phi)Y^*_{\mu,\nu}(\theta_D,\phi_D), \tag{5}$$

where θ and ϕ (θ_D and ϕ_D) are the polar angles of the electron (impurity atom), and $f_\mu(r)$ is

$$f_\mu(r) = \begin{cases} \frac{1}{D}(\frac{r}{D})^\mu, & r \leq D \\ \frac{1}{r}(\frac{D}{r})^\mu, & r \geq D \end{cases}. \tag{6}$$

As the distance between the donors becomes very large ($D \to \infty$), we can see that the coupling between the two impurities is weak and they behave like two separate isolated hydrogenic impurities. But when D is very small ($D \to 0$), the coupling between the two impurities will be very large and the total potential energy is very similar to the potential energy of an electron around a single dopant with a double doping charge, i.e. the He^+ atom-like impurity state.

If the lengths and energies are taken in terms of the effective Bohr radius ($a_B = \frac{\hbar^2\varepsilon}{m^* e^2}$) and the effective Rydberg constant ($R_y^* = \frac{\hbar^2}{2m^* a_B^2}$), respectively, the total Hamiltonian is obtained in dimensionless form

$$H = -\nabla^2 + V_{QD}(r) + \frac{2}{D} - 2Z\left(\sum_{\mu} \frac{4\pi}{2\mu+1} f_\mu(r) \sum_{\nu=-\mu}^{\mu} Y^*_{\mu,\nu}(\theta,\phi) Y^*_{\mu,\nu}(\theta_D,\phi_D) + \frac{1}{r}\right), \quad (7)$$

where ∇^2 is the Laplace operator.

To determine the energy eigenvalues and eigenfunctions of the system, we must solve the Schrödinger equation

$$H\psi_{nlm}(r,\theta,\phi) = E_{nlm}\psi_{nlm}(r,\theta,\phi)\,, \quad (8)$$

where n is the principal, l is the angular momentum and m ($-l \le m \le l$) is the magnetic momentum quantum numbers. This equation is not analytically solvable, so we use the diagonalization method to calculate the eigenfunctions and corresponding eigenvalues. Therefore, we choose a linear combination of trial envelope wavefunctions representing the electron in the infinite spherical QD (Al et al. 2021)

$$\psi_{nlm}(r,\theta,\phi) = \sum_j c_{n_j,l_j} \psi^{(0)}_{n_j l_j m}(r,\theta,\phi), \quad (9)$$

where c_{n_j,l_j} are the expansion coefficients, $\psi^{(0)}_{n_j l_j m}(r,\theta,\phi)$ is the total wavefunction describing the motion of the electron without impurity atoms and it is written in terms of radial wavefunction and spherical harmonics due to the spherical symmetry of the system as

$$\psi^{(0)}_{nlm}(r,\theta,\phi) = \varphi^{(0)}_{nl}(r) Y_{lm}(\theta,\phi), \quad (10)$$

where the radial wave function-$\varphi^{(0)}_{nl}(r)$ is given as

$$\varphi^{(0)}_{nl}(r) = \begin{cases} N j_l(k_{nl} r), & r < R_i \\ 0, & r \ge R_i \end{cases}, \quad (11)$$

where R_i ($R_i >> R$) is the radius of the infinite spherical QD, N is the normalization constant and k_{nl} is the nth root of lth order spherical Bessel functions. The size of the series expansion in Eq. 9 is readjusted to get results with an accuracy of 0.01 meV for each energy value.

Since the ionization process is $D_2^+ \rightarrow D^+ + D^+ e^-$, the binding energy of D_2^+ is given by

$$E^b_{nlm} = E_{nlm}(Z=0) - E_{nlm}(Z=1), \quad (12)$$

where $E_{nlm}(Z=0)$ and $E_{nlm}(Z=1)$ are the energies without and with electron-donor interactions, respectively.

2.2 Linear and nonlinear optical absorption

The optical transition that occurs by the absorption of a photon between the initial and final states is known as the photo-absorption method. As electromagnetic radiation passes

through the QD, OACs provide information about the reduction in radiation intensity. To calculate the various optical properties, we need to consider the interaction between the polarized electromagnetic wave with angular frequency ω and the QD ensemble (Fermi's Golden Rule) (Rezaei et al. 2011).

OAC is considered an important parameter for optical transitions. To investigate OACs, the optical transition energy between the two states studied is calculated. Using the density matrix formalism, the analytical expression of the linear OAC for a two-level quantum system interacting with a monochromatic optical field is given by

$$\alpha^{(1)}(\omega) = \sqrt{\frac{\mu}{\varepsilon_r}} \frac{\sigma_s \Gamma_{ij}}{(E_{ij} - \hbar\omega)^2 + (\hbar\Gamma_{ij})^2} \hbar\omega |M_{ij}|^2, \tag{13}$$

where $\mu = \frac{1}{\varepsilon_0 c^2}$ is the magnetic permeability of the system (ε_0 and c are the permittivity and light speed of the vacuum), $\varepsilon_r = n_r^2 \varepsilon_0$ is the real part of the dielectric permittivity of the material, n_r is the static component of the refractive index in QD, σ_s is the electron density of the QD, non-diagonal matrix element Γ_{ij} is the phenomenological relaxation ratio operator caused by electron-phonon, electron-electron and other collision processes and it is the inverse of relaxation time-τ_{ij}, $E_{ij} = E_j - E_i$ is the energy difference between the levels in two level systems, $\hbar\omega$ is the energy of the incident photon and M_{ij} are the dipole moment matrix elements between the initial and final states in QD and they can be calculated from

$$M_{ij} = \langle \psi_i | er \cos\theta | \psi_j \rangle, \tag{14}$$

where ψ_i and ψ_j are wave functions representing the electron at the initial and final levels.

Since the nonlinear optical absorption applies at very high radiation intensities, the nonlinear OAC which is derived from density matrix equations using perturbation theory can lead to misleading results, such as the bleaching effect and even negative absorption. In order to obtain a nonlinear OAC without using perturbation theory, Zaluzny used a steady state solution of the relevant density matrix equations, under the usual rotating wave approximation (Załużny 1993). Recently, Paspalakis et al. have studied on the nonlinear optical absorption and nonlinear optical rectification in an asymmetric semiconductor QD structure under a strong probe field excitation using extended version of the rotating wave approximation (Paspalakis et al. 2013). As a result of this study, they obtained the nonlinear OAC as

$$\alpha^{(3)}(\omega) = \frac{E_{ij}\sigma_s |M_{ij}|^2 T_2}{\varepsilon_0 n_r c} \frac{\left| J_0^2\left(\frac{|M_{ii} - M_{jj}|E_0}{\hbar\omega}\right) - J_2^2\left(\frac{|M_{ii} - M_{jj}|E_0}{\hbar\omega}\right) \right|}{1 + T_2^2(\hbar\omega - E_{ij})^2 + |M_{ij}|^2 E_0^2 T_1 T_2}, \tag{15}$$

where J_n is the nth order Bessel function, $E_0 = \sqrt{\frac{I}{2\varepsilon_0 n_r c}}$ is the amplitude of the incident light (I is the intensity of the incident light), T_1 is population decay (longitudinal relaxation) time and T_2 is dephasing (transverse relaxation) time.

For linear OAC the resonance condition is $\hbar\omega = \sqrt{E_{ij}^2 + (\hbar\Gamma_{ij})^2}$ (Al et al. 2021). In this case, the maximum value of linear OAC is given by

$$\alpha^{(1)}(\omega) = \sqrt{\frac{\mu}{\varepsilon_r}} \frac{e^2 \sigma_s \Gamma_{ij}}{(E_{ij} - \hbar\omega)^2 + (\hbar\Gamma_{ij})^2} \Omega, \tag{16}$$

where $\Omega = e^{-2}\sqrt{E_{ij}^2 + (\hbar\Gamma_{ij})^2}|M_{ij}|^2$ is the main parameter that determine the amplitude of the linear OAC. On the other hand, the $M_{jj} - M_{ii}$ term causes a small effect on the nonlinear OAC around the resonance when any of the donor atoms is outside the center of the QD. However, this term must be taken into account when considering its essential roles on incident photon energies outside the resonance region. In the case of $M_{jj} - M_{ii} = 0$, the maximum value of nonlinear OAC is given by

$$\alpha^{(3)}(\omega) = \frac{E_{ij}\sigma_s|M_{ij}|^2T_2}{\varepsilon_0 n_r c}\frac{1}{1 + T_2^2(\hbar\omega - E_{ij})^2 + |M_{ij}|^2E_0^2T_1T_2}. \tag{17}$$

According to the minimum energy rule, not every possible transition in the absorption spectrum can be observed. In addition to the conservation of energy, the conservation of angular momentum and some symmetry rules must also be provided. Due to the azimuth symmetry of the system and the property of spherical harmonics, dipole transitions in spherical QDs are only allowed between states satisfying the $\Delta l = \pm 1$ and $\Delta m = 0, \pm 1$ selection rules. The selection rules determine the final state of the electron after absorption. All allowed transitions are included in the dipole matrix elements, i.e. optical transitions are allowed when the dipole matrix element is not zero. In this study, we only considered $m = 0$ states.

3 Results and discussion

At this stage, we report the obtained energy states, binding energy and intersubband OACs of a D_2^+ complex confined in a spherical QD with finite confinement potential for different values of the QD size and internuclear distance values. The used physical parametres are: $\varepsilon = 13.18$, $a_B = 10.4\,\text{nm}$, $R_y^* = 5.23\,\text{meV}$, $V_0 = 224.46\,\text{meV}$, $m^* = 0.067m_0$ (where $m_0 = 9.10956 \times 10^{-31}\,\text{kg}$ is the mass of free electron), $T_{ij} = 0.14\,\text{ps}$, $T_1 = 10\,\text{ps}$, $T_2 = 5\,\text{ps}$, $\mu = 4\pi \times 10^{-7}\,\text{H/m}$, $n_r = 3.63$, $\sigma_s = 1 \times 10^{23}\,\text{m}^{-3}$ and $I = 400\,\text{MW/m}^2$.

In Fig. 1, we display variation of the total energy of the D_2^+ complex (total energy of the electron plus the donor–donor Coulomb repulsion) corresponding to the $1s$ and $1p$ states as a function of the internuclear distance for four different values of QD size ($R = 10,\ 30,\ 50$ and 100 nm). From this figure, in the bound case, i.e., the total energy< 0, it is possible to conclude that increasing the QD size leads to greater dissociation energy and greater internuclear equilibrium distance for the $1s$ state. Such that for $R = 30$ nm the internuclear equilibrium distance and dissociation energy corresponding to the $1s$ state are respectively 9 nm and 1.73 meV while for $R = 100\ nm$ these values get to be 11 nm and 2.51 meV. This means that as the QD width decreases, the kinetic energy of the electron increases and becomes more energetic, therefore the D_2^+ complex gets to be disassociated. These results are in agreement with those previously reported in the study by Suaza et al. (2018). It is apparent that similar behavior is in question for the equilibrium distance corresponding to the $1p$ state. On the other hand, depending on the symmetry of the wave function related to the 1p state the dissociation energy decreases with QD size. Nevertheless, for each value of R considered, the $1p$ state is lying above the $1s$ state. The effect of QD size on the electronic structure of the D_2^+ complex is seen in more detail in Table 1. Comparing the variation of the $1s$ and $1p$ states, it appears that the QD dimension-R is more influential on the equilibrium distance related to the $1p$ state. Also, notice that for sufficiently large QD

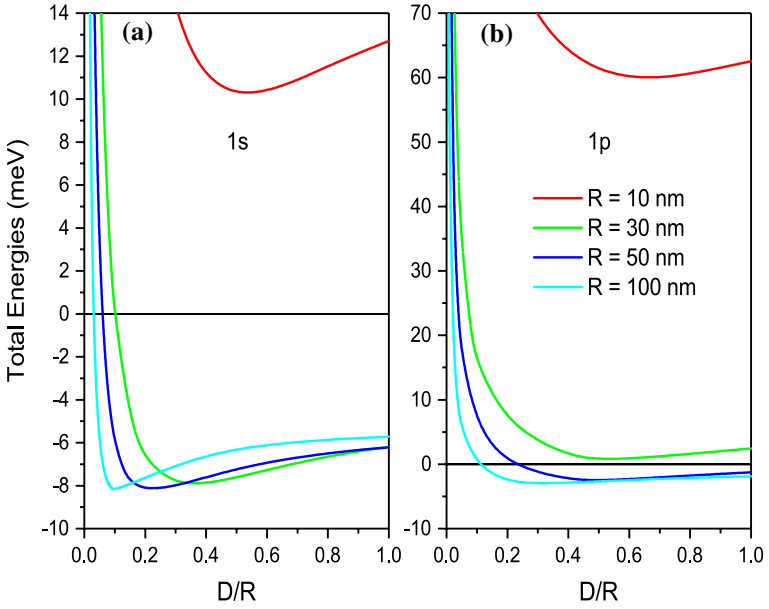

Fig. 1 (color online) Variation of the total energies of the D_2^+ complex corresponding to the (**a**) 1*s* and (**b**) 1*p* states as a function of internuclear distance for four different QD size values ($R = 10$, 30, 50 and 100 nm)

Table 1 Effect of QD size on the electronic structure of the D_2^+ complex

Quantum size	Equilibrium distance	1*s*	Equilibrium distance	1*p*
R (nm)	*D* (nm)	Dissociation energy (meV)	*D* (nm)	Dissociation energy (meV)
10	5	2.4889	7	2.5706
30	9	1.73215	15	1.66607
50	10	1.98825	25	1.23604
100	11	2.51194	30	1.11851

width values, the effect of the geometric confinement negligibly weakens while that of the nuclear would buildup. Therefore, in the case of sufficiently large internuclear distance and QD width values (for sufficiently large values of both *R* and *D* parameters), the D_2^+ complex turns into two isolated donor atoms with the sole electron ending up on one of the two nuclei.

The variation of binding energies corresponding to the 1*s* and 1*p* states of the D_2^+ complex as a function of the QD radius-*R* is presented in Fig. 2 for several different values of the internuclear distance. As can be clearly seen in the figure, for all *D* values considered, the binding energy corresponding to the 1*s* and 1*p* states reaches its maximum value at about $R = 8$ nm. The reason for this is that when QD is at this width

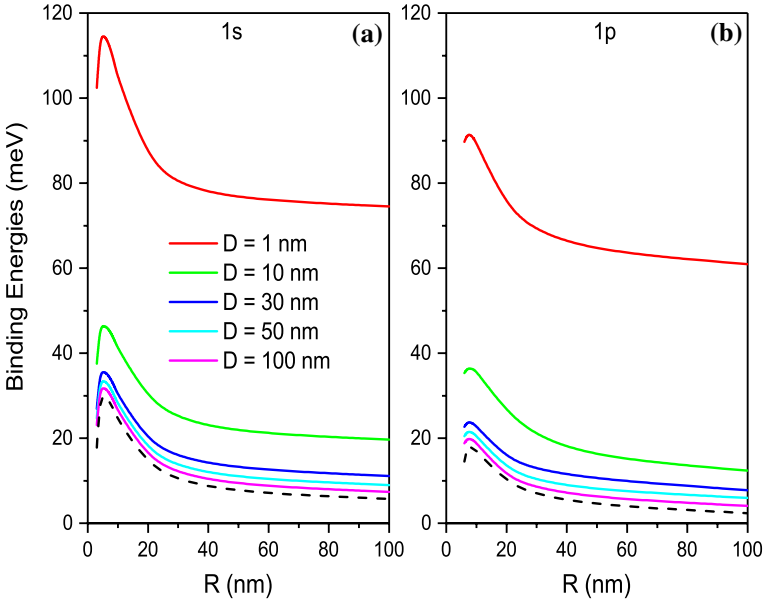

Fig. 2 (color online) Variation of binding energies corresponding to the (**a**) $1s$ and (**b**) $1p$ states of the D_2^+ complex as a function of QD radius-R for several different values of the internuclear distance. The dashed line indicates the binding energy of the single impurity-D^0

value, the spatial confinement takes its strongest value. On the other hand, another point that should be emphasized is that in cases where the internuclear distance parameter-D is very small, since the internal potential barrier between Coulomb centers is sufficiently narrow and low, the electron is shared by both impurity atoms. Therefore, in this case the molecular complex is more stable and the binding energy is large enough. Also note that when the distance between impurity atoms is large enough, the D_2^+ complex is reduced to a single isolated hydrogenic impurity atom case. Thus, in this case, the binding energies corresponding to the $1s$ and $1p$ states converge to the D^0 binding energies, as can be clearly seen from the figure. For example, in the case of $D = 100$ nm, and $R = 100$ nm, the binding energy value corresponding to the $1s$ state is $E_b = 1.4R_y^*$. These assessments show that the method we used in the present study provides a realistic description of the energy spectrum of the D_2^+ complex confined in a spherical QD.

In Figs. 3 and 4, we show the evolution of the linear and third-order nonlinear intersubband ($1s \rightarrow 1p$) OACs related to the D_2^+ complex confined in a spherical QD for different values of the confinement size-R and internuclear distance-D, respectively. In general, as the value of nuclear distance increases, it is observed that for narrow QDs the peak position of OACs shifts towards larger photon energies, whereas for wider QDs it is redshifted. We can clarify this feature as follows: Since the $1p$ energy state in narrow QDs is rather large compared to the $1s$ state, this state is less affected by the change of the Coulombic potential term in the base of the geometric confinement than the $1s$ state. Therefore, as can be seen in Fig. 1, the $1s$ energy state changes to a greater rate with increasing internuclear distance-D than the $1p$ state, resulting in a significant increase in the energy difference-E_{ij}. However, in large QDs where the quantum confinement is weak, both energy states change almost at the same rate and accordingly, the energy difference-E_{ij} decreases as the internuclear

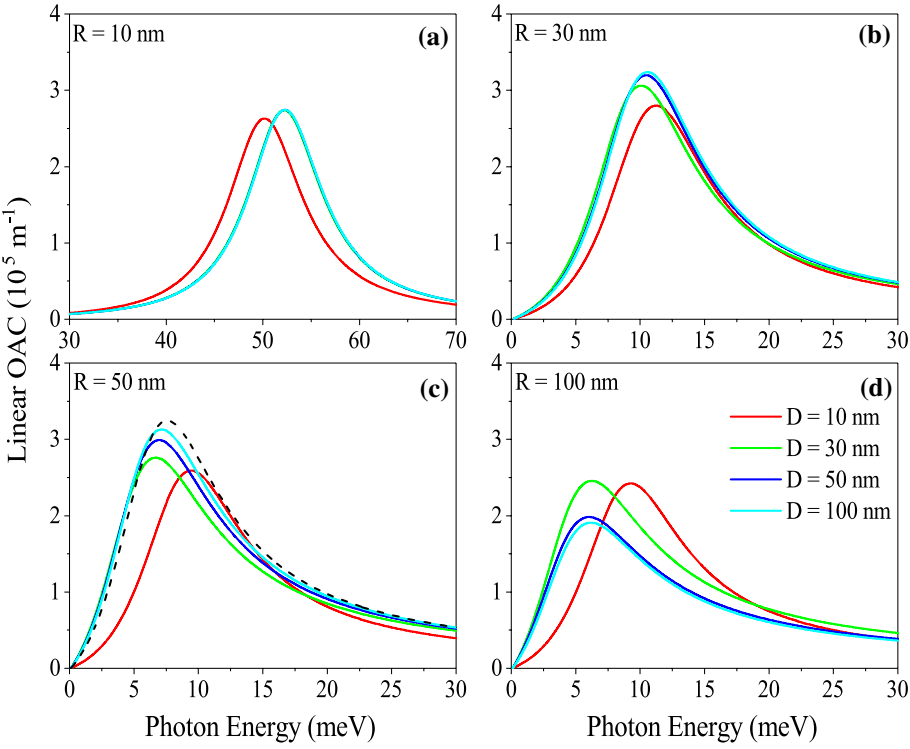

Fig. 3 (color online) Variation of linear intersubband ($1s \rightarrow 1p$) OAC with respect to incident photon energy related to the D_2^+ complex confined in a spherical QD for different values of confinement size-R and internuclear distance-D. The dashed line indicates the linear absorption coefficient of the single impurity-D^0

distance increases. To illustrate this behavior in more detail, the variation of the related energy difference-E_{ij} is presented in Fig. 5a as a function of internuclear distance. It is apparent that as mentioned above in the strong confinement regime, the energy difference-E_{ij} increases with the distance between nuclei, but the opposite behavior is observed in the case of weak geometric confinement. In addition, in accordance with the evaluations made above, the energy difference-E_{ij} converges to the single-impurity-D^0 results at sufficiently large R and D values. By analyzing Figs. 3 and 4 in detail, especially at large R values, it has been found that the amplitudes of linear and third-order nonlinear OACs change significantly as D increases. In order to visualize the variation in the amplitude of the linear OAC depending on the QD size and internuclear distance, the variation of the Ω factor is presented in Fig. 5 (b) as a function of the parameter-D. As can be seen in this figure, while the Ω factor which affects the peak amplitude of the linear OAC decreases with increasing values of D for $R = 100\ nm$, it increases significantly for the other values of R considered. Based on these results, it can be concluded that the QD size and internuclear distance have significant influence on the optoelectronic properties of the D_2^+ complex confined in a spherical QD.

Before concluding the discussion, another point that we would like to emphasize is this: The realistic self-assembled QDs are not spherical. Their realistic form of the non-flat self-assembled QDs is truncated pyramidal, in which a dot of one material is coherently

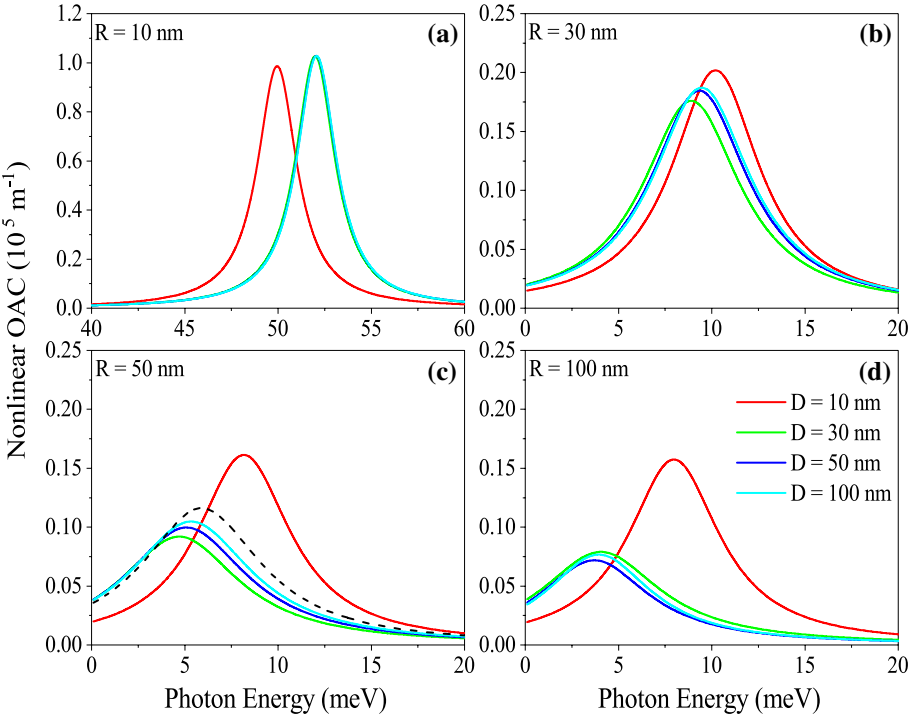

Fig. 4 (color online) Variation of third-order nonlinear intersubband ($1s \rightarrow 1p$) OAC with respect to incident photon energy related to the D_2^+ complex confined in a spherical QD for different values of confinement size-R and internuclear distance-D. The dashed line indicates the third-order nonlinear linear absorption coefficient of the single impurity-D^0

strained in a matrix of another material. It turns out that in such heterostructures the biaxial strain is a function of position, decaying with distance away from the interface. Such a behavior can modify the confining potential, leading to carrier localization (Williamson et al. 1998; Wang 2001). The existence of position-dependent strain in non-flat heterostructures can control the electronic properties, leading, for example, to interfacial localization of energy states on the interface of matrix-embedded dots and the shape of dot can control the level sequence and degeneracy (He et al. 2004). Moreover, large ensembles of self-assembled QDs in practice has size dispersion and hence inhomogeneous broadening. As a corollary to this feature, the size of the molecules will not be the same in all QDs. The broadening of the photoluminescence emission peaks is generally attributed to QD nonuniformity. Theoretical calculations have shown that the QD height, rather than the diameter, the volume, the composition, or the strain, appears to be the key parameter that controls the inhomogeneous broadening of the optical transitions Perret et al. (2000).

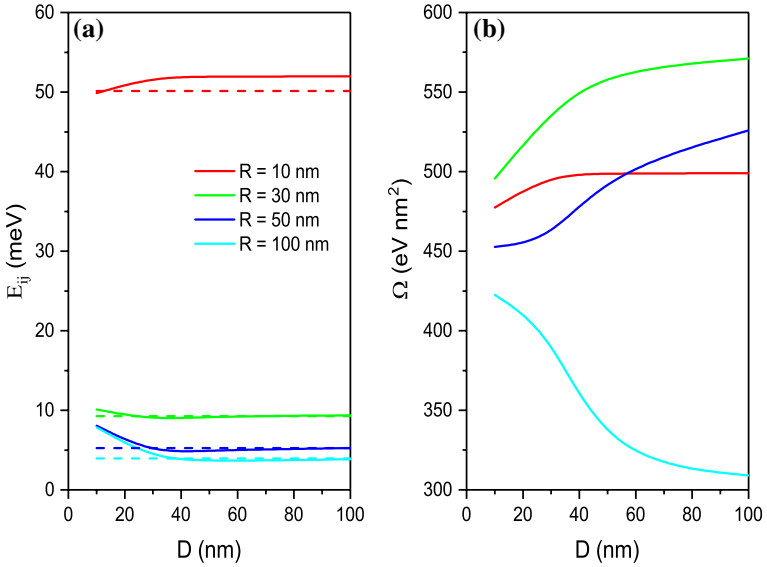

Fig. 5 (color online) Variation of E_{ij} and Ω factor depending on QD size and internuclear distance. The dashed lines indicate the single impurity-D^0 case

4 Conclusions

We have performed a theoretically study on the energy spectrum and optical intersubband transitions of the D_2^+ complex confined in a spherical QD. We analyzed the effect of the QD size and internuclear distance on the binding energy, equilibrium distance and optical response of the singly ionized double donor complex. Theoretical analysis of the D_2^+ system indicated that the internuclear distance significantly affects the energy difference between the two lowest-lying electron states and amplitude of the optical absorption, especially in the case of the weak quantum confinement regime. The internuclear distance and QD size dependence of the low-lying energy spectrum of the D_2^+ complex in a QD favors the tuning of the interlevel transitions within the conduction band of an appropriate two-level system. Also, in the case of sufficiently large internuclear distance and QD size, the binding energy, OACs and the energy difference-E_{ij} tend to those of single-impurity-D^0.

Funding The authors have not disclosed any funding.

Availability of data and materials This manuscript has associated data in a data repository.

Declarations

Conflicts of interest The authors do not have any financial and non-financial competing interests statement.

References

Aassime, A., Johansson, G., Wendin, G., Schoelkopf, R.J., Delsing, P.: Radio-frequency single-electron transistor as readout device for qubits: charge sensitivity and backaction. Phys. Rev. Lett. **86**, 3376–3379 (2001)

Abolfath, R.M.: Para-ortho transition of artificial H_2 molecule in lateral quantum dots doped with magnetic impurities. Phys. Rev. B **80**, 165332 (2009)

Adachi, S.: GaAs, AlAs, and $Al_xGa_{1-x}As$: material parameters for use in research and device applications. J. Appl. Phys. **58**, R1–R29 (1985)

Al, E.B., Kasapoglu, E., Sari, H., Sökmen, I.: Optical properties of spherical quantum dot in the presence of donor impurity under the magnetic field. Physica B **613**, 412874 (2021)

Al, E.B., Kasapoglu, E., Sari, H., Sökmen, I.: Zeeman splitting, Zeeman transitions and optical absorption of an electron confined in spherical quantum dots under the magnetic field. Phil. Mag. **101**, 117–128 (2021)

Barrett, S.D., Milburn, G.J.: Electric-field driven donor-based charge qubits in semiconductors. Phys. Rev. B **68**, 155307 (2003)

Bednarek, S., Szafran, B., Adamowski, J.: Many-electron artificial atoms. Phys. Rev. B **59**, 13036–13042 (1999)

Bera, A., Ganguly, J., Saha, S., Ghosh, M.: Interplay between noise and position-dependent dielectric screening function in modulating nonlinear optical properties of impurity doped quantum dots. Optik **127**, 6771–6778 (2016)

Bimberg, D., Grundmann, M., Ledentsov, N.: Quantum Dot Heterostructures, p. 344. Wiley, Chichester (1999)

Calderón, M.J., Koiller, B., Hu, X., Das Sarma, S.: Quantum Control of Donor Electrons at the Si/SiO_2 Interface. Phys. Rev. Lett. **96**, 096802 (2006)

Calderón, M.J., Koiller, B., Das Sarma, S.: External field control of donor electron exchange at the Si/SiO_2 interface. Phys. Rev. B **75**, 125311 (2007)

Cheng, S.-J., Sheng, W., Hawrylak, P.: Theory of excitonic artificial atoms: InGaAs/GaAs quantum dots in strong magnetic fields. Phys. Rev. B **68**, 235330 (2003)

Du, M.-H., Erwin, S.C., Efros, A.L.: Trapped-dopant model of doping in semiconductor nanocrystals. Nano Lett. **8**, 2878–2882 (2008)

Fuhrer, A., Füchsle, M., Reusch, T.C.G., Weber, B., Simmons, M.Y.: Atomic-scale, all epitaxial in-plane gated donor quantum dot in silicon. Nano Lett. **9**, 707–710 (2009)

Ghosh, A.P., Mandal, A., Sarkar, S., Ghosh, M.: Influence of position-dependent effective mass on the nonlinear optical properties of impurity doped quantum dots in presence of Gaussian white noise. Opt. Commun. **367**, 325–334 (2016)

He, L., Bester, G., Zunger, A.: Strain-induced interfacial hole localization in self-assembled quantum dots: compressive InAs/GaAs versus tensile InAs/InSb. Phys. Rev. B **70**, 235316 (2004)

Hollenberg, L.C.L., Dzurak, A.S., Wellard, C., Hamilton, A.R., Reilly, D.J., Milburn, G.J., Clark, R.G.: Charge-based quantum computing using single donors in semiconductors. Phys. Rev. Lett. **69**, 113301 (2004)

Kang, S., Liu, Y.-M., Shi, T.-Y.: The characteristics for H_2^+-like impurities confined by spherical quantum dots. Eur. Phys. J. B **63**, 37–42 (2008a)

Kang, S., Liu, Y.-M., Shi, T.-Y.: H_2^+-Like impurities confined by spherical quantum dots: a candidate for charge qubits. Commun. Theor. Phys. **50**, 767–770 (2008b)

Koiller, B., Hu, X., Das Sarma, S.: Electric-field driven donor-based charge qubits in semiconductors. Phys. Rev. B **73**, 045319 (2006)

Makkara, M., Viswanatha, R.: Frontier challenges in doping quantum dots: synthesis and characterization. RSC Adv. **8**, 22103–22112 (2018)

Manjarres-García, R., Escorcia-Salas, G.E., Mikhailov, I.D., Sierra-Ortega, J.: Singly ionized double-donor complex in vertically coupled quantum dots. Nanoscale Res. Lett. **7**, 489 (2012)

Matsukawa, T., Fukai, T., Suzuki, S., Hara, K., Koh, M., Ohdomari, I.: Development of single-ion implantation—Controllability of implanted ion number. Appl. Surf. Sci. **117–118**, 677–683 (1997)

Movilla, J.L., Ballester, A., Planelles, J.: Coupled donors in quantum dots: quantum size and dielectric mismatch effects. Phys. Rev. B **79**, 195319 (2009)

O'Brien, J.L., Schofield, S.R., Simmons, M.Y., Clark, R.G., Dzurak, A.S., Curson, N.J., Kane, B.E., McAlpine, N.S., Hawley, M.E., Brown, G.W.: Towards the fabrication of phosphorus qubits for a silicon quantum computer. Phys. Rev. B **64**, 161401(R) (2001)

Openov, L.A.: Resonant pulse operations on the buried donor charge qubits in semiconductors. Phys. Rev. B **70**, 233313 (2004)

Paspalakis, E., Boviatsis, J., Baskoutas, S.: Effects of probe field intensity in nonlinear optical processes in asymmetric semiconductor quantum dots. J. Appl. Phys. **114**, 153107 (2013)
Pavlović, V.: Electromagnetically induced transparency in a spherical quantum dot with hydrogenic impurity in a four level ladder configuration. Optik **127**, 6351–6357 (2016)
Perret, N., Morris, D., Franchomme-Fossé, L., Côté, R., Fafard, S., Aimez, V., Beauvais, J.: Origin of the inhomogenous broadening and alloy intermixing in InAs/GaAs self-assembled quantum dots. Phys. Rev. B **62**, 5092 (2000)
Rezaei, G., Vahdani, M.R.K., Vaseghi, B.: Nonlinear optical properties of a hydrogenic impurity in an ellipsoidal finite potential quantum dot. Curr. Appl. Phys. **11**, 176–181 (2011)
Schoelkopf, R.J., Wahlgren, P., Hozhevnikov, A.A., Delsing, P., Prober, D.E.: The radio-frequency single-electron transistor (RF-SET): a fast and ultrasensitive electrometer. Science **280**, 1238–1242 (1998)
Schofield, S.R., Curson, N.J., Simmons, M.Y., Ruess, F.J., Hallam, T., Oberbeck, L., Clark, R.G.: Atomically precise placement of single dopants in Si. Phys. Rev. Lett. **91**, 136104 (2003)
Shinada, T., Kurosawa, T., Kobayashi, T., Nakayama, H., Ohdomari, I.: Control of both number and position of dopant atoms in semiconductors by single ion implantation. In: International Workshop on Junction Technology, pp. 16–20 (2006)
Shinada, T., Ishikawa, A., Hinoshita, C., Koh, M., Ohdomari, I.: Reduction of fluctuation in semiconductor conductivity by one-by-one ion implantation of dopant atoms. Jpn J. Appl. Phys. **39**, L265–L268 (2000)
Shinada, T., Koyama, H., Hinoshita, C., Imamura, K., Ohdomari, I.: Improvement of focused ion-beam optics in single-ion implantation for higher aiming precision of one-by-one doping of impurity atoms into nano-scale semiconductor devices. Jpn J. Appl. Phys. **41**, L287–L290 (2002)
Shinada, T., Okamoto, S., Kobayashi, T., Ohdomari, I.: Enhancing semiconductor device performance using ordered dopant arrays. Nature **437**, 1128–1131 (2005)
Suaza, Y.A., Laroze, D., Fulla, M.R., Marín, J.H.: D_2^+ molecular complex in non-uniform height quantum ribbon under crossed electric and magnetic fields. Chem. Phys. Lett. **699**, 267–274 (2018)
Tsukanov, A.V.: Single-qubit operations in the double-donor structure driven by optical and voltage pulses. Phys. Rev. B **76**, 035328 (2007)
Wang, L.-W.: Calculations of carrier localization in $In_xGa_{1-x}N$. Phys. Rev. B **63**, 245107 (2001)
Williamson, A.J., Zunger, A., Canning, A.: Prediction of a strain-induced conduction-band minimum in embedded quantum dots. Phys. Rev. B **57**, R4253 (1998)
Wu, J., Chen, S., Seeds, A., Liu, H.: Quantum dot optoelectronic devices: lasers, photodetectors and solar cells. J. Phys. D: Appl. Phys. **48**, 363001 (2015)
Xu, H., Li, Z., He, F., Wang, X., Atia-Tul-Noor, A., Kielpinski, D., Sang, R.T., Litvinyuk, I.V.: Observing electron localization in a dissociating H2+ molecule in real time. Nat. Commun. **8**, 15849 (2017)
Załużny, M.: Saturation of intersubband absorption and optical rectification in asymmetric quantum wells. J. Appl. Phys. **74**, 4716 (1993)